Organic & Biomolecular Chemistry

RSC Publishing

PAPER

View Article Online
View Journal | View Issue

Synthesis and properties of 2′-*O*-neopentyl modified oligonucleotides†

Cite this: *Org. Biomol. Chem.*, 2013, **11**, 1345

Gérald Mathis,[a,b] Stéphane Bourg,[a,c] Samia Aci-Sèche,[a] Jean-Christophe Truffert[b] and Ulysse Asseline*[a]

Received 23rd September 2012,
Accepted 10th December 2012

DOI: 10.1039/c2ob26871j

www.rsc.org/obc

2′-*O*-Neopentyldeoxyuridine (Un) was synthesized and incorporated into a series of oligodeoxyribonucleotides. Single and triple incorporations in various arrangements were performed. The Watson and Crick pairing properties with complementary DNA and RNA were investigated by UV melting curves, CD spectroscopy, and molecular dynamic simulations. The results were compared to those obtained with DNA–DNA and DNA–RNA duplexes involving dU at the same positions. Oligonucleotides containing Un clearly demonstrated their ability to form duplexes with both complementary DNA and RNA but with higher stabilities for the DNA–RNA duplexes similar to the one of the parent DNA–RNA duplex. Investigations into the thermodynamic properties of these 17-base-pair duplexes revealed ΔG values (37 °C) that are in line with the measured T_m values for both the DNA–DNA and DNA–RNA duplexes. CD spectroscopic structural investigations indicated that the conformations of the DNA–DNA and DNA–RNA duplexes involving Un are similar to those of the dT–rA and dU–rA containing duplexes. Only small changes in intensities and weak blue shifts were observed when three Uns were incorporated into the duplexes. The results of the molecular dynamic simulations showed, for the six duplexes involving the modified nucleoside Un, calculated curvatures similar to those of the corresponding unmodified duplexes without base-pair disruption. The neopentyl group is able to be accommodated in the minor grooves of both the DNA–DNA and RNA–DNA duplexes. However, molecular dynamic simulations indicated that the Uns adopt a C2′-*exo* sugar pucker conformation close to an A-helix type without perturbing the C2′-*endo* sugar pucker conformations of their 2′-deoxynucleoside neighbours. These results confirm the potential of 2′-*O*-neopentyldeoxyuridine as a nucleoside surrogate for oligonucleotide based therapeutic strategies.

Introduction

Chemically modified oligonucleotides (ONs) are powerful research tools for gene structure, regulation and function analysis as well as promising therapeutic agents.[1–13] It Has been known for decades that modulation of gene expression can be achieved by targeting messenger RNAs with single-stranded chemically modified ONs (antisense-strategy).[14] More recently, it has been demonstrated that inhibition of gene expression in mammalian cells can be efficiently achieved by double-stranded oligoribonucleotides *via* the interference (RNAi) pathway.[15] RNA interference involves complex biological gene-silencing mechanisms and homogeneously increased stability of chemically modified oligoribonucleotides to their target may reduce their efficiency by impairing guide strand dissociation. In addition to the common properties (resistance to nucleases, cell-specific delivery, efficient uptake and adequate intracellular distribution), efficient double-stranded chemically modified siRNAs require fine tuning of their binding affinity along the sequences. The rapid development of this strategy has benefited from the different structural modifications of ONs previously selected for the antisense strategy and potent siRNA have been selected.[16–33] However, this strategy triggers unintended gene silencing due to the inherent miRNA-like behaviour of double-stranded RNAs. It has been recently shown that chemical modifications of siRNAs at specific positions can reduce off-targeting.[8,22–27,30,32] The most efficient is the strongly destabilizing unlocked nucleic acid (UNA).[26] A few modifications have been tested. We do believe that other new chemically modified nucleosides, to

[a]*Centre de Biophysique Moléculaire UPR 4301 CNRS, Conventionnée avec l'Université d'Orléans, Rue Charles Sadron, 45071 Orléans Cedex 02, France. E-mail: ulysse.asseline@cnrs-orleans.fr; Fax: +33-2-38-63-15-17*
[b]*NucleoSyn. Pépinières d'entreprises – Centre Innovation 16, Rue Léonard de Vinci, 45074 Orléans Cedex 2, France*
[c]*Institut de Chimie Organique et Analytique, Université d'Orléans, UMR 7311 CNRS, rue de Chartres, 45067 Orléans Cedex 2, France*

†Electronic supplementary information (ESI) available: ^{1}H NMR, ^{13}C NMR, ^{31}P NMR spectra. HPLC and MS characterisations for ONs and Fig. 6–8. See DOI: 10.1039/c2ob26871j

be identified, may be used to finely tune the hybridization properties of chemically modified siRNA. Previous studies indicated that 2′-modified ONs appear to be promising due to their favourable hybridization with complementary RNA.[6,16,17,30–37] More often, such modifications force the ONs to adopt a higher proportion of the northern conformation in a helical structure, which is one of the contributing factors of the stronger hybridization property of these modified ONs. The binding affinity of the modified ONs is also dependent on the size of the alkoxy group. We focused on the neopentyl group that to our knowledge has never been reported for 2′-substitution of nucleosides. We made the hypothesis that this bulky group could be accommodated in the minor groove upon hybridization of the ON with its RNA target.

Here, we report the synthesis of 2′-*O*-neopentyldeoxyuridine (Un) and study the effect of its single and multiple incorporations, in different arrangements, into a series of 17-mer oligodeoxyribonucleotides on their binding properties with DNA and RNA targets. The thermal and thermodynamic transition profiles of duplexes with complementary DNA and RNA were evaluated. Owing to the structural differences between Un and dT, in order to assess the contribution of the 2′-*O*-neopentyl group to duplex stability, a series of ONs involving dU in the same positions was also studied. A study of the helix conformation of duplexes with different Un contents was carried out by CD spectroscopy and molecular dynamic simulations.

Results and discussion

Structures and experimental design

The neopentyl group was linked to the 2′-position of 2′-deoxyuridine and the modified nucleoside was incorporated in various arrangements into a 17-mer sequence (Fig. 1 and 2). A single incorporation was performed at either the 5′-end or the internal position of the sequence (ONs **4** and **5**). Multiple insertions (three) were performed either in a continuous row (ON **6**) or spaced by natural nucleosides (ON **7**). For a comprehensive comparison of the properties of the new modified nucleoside, the binding properties of ONs involving either one (ONs **8** and **9**) or three dU incorporations (ONs **10** and **11**) at the same positions along with the unmodified ON (ON **3**) used as a reference were also studied. 23-mer DNA (ON **1**) and RNA (ON **2**) targets were chosen so that, upon hybridization, three nucleotides would overhang on each side of the duplexes in order to mimic the interaction of ONs with full length targets.[38,39] The structures of the modified nucleosides Un and dU used in this study are shown in Fig. 1 and those of the ONs **1–11** are depicted in Fig. 2.

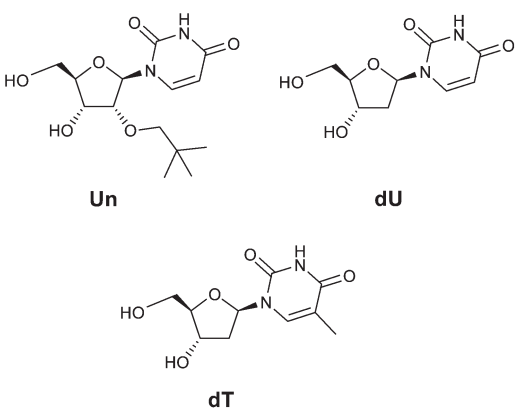

Fig. 1 Chemical structures of 2′-*O*-neopentyldeoxyuridine (Un), 2′-deoxyuridine (dU) and thymidine (dT).

ON	Sequence
1	5′ d-(TAC ACT AAA **X**CT GGT AAC AAC TC) 3′
2	5′ r-(UAC ACU AAA **X**CU GGU AAC AAC UC) 3′
3	5′ d-(TTG TTA CCA GTT TTA GT) 3′
4	5′ d-(**Un**TG TTA CCA GTT TTA GT) 3′
5	5′ d-(TTG TTA CCA G**Un**T TTA GT) 3′
6	5′ d-(TTG TTA CCA G**UnUn Un**TA GT) 3′
7	5′ d-(TTG T**Un**A CCA G**Un**T T**Un**A GT) 3′
8	5′ d-(**dU**TG TTA CCA GTT TTA GT) 3′
9	5′ d-(TTG TTA CCA G**dU**T TTA GT) 3′
10	5′ d-(TTG TTA CCA G**dUdU dU**TA GT) 3′
11	5′ d-(TTG T**dU**A CCA G**dU**T T**dU**A GT) 3′
	X = A, C, G or T

Fig. 2 Sequences of the DNA and RNA targets **1** and **2**, the reference ON **3** and the modified ONs **4–11**.

Synthesis

Synthesis of the 2′-*O*-neopentyldeoxyuridine and its phosphoramidite building block. Several methods for the 2′-alkylation of uridine have been reported previously. Most of them include the protection of 5′- and 3′-hydroxyl groups as well as the N-3 position of the nucleic base to make the alkylation of the 2′-position specific.[40,41] We chose to proceed without protection of the nucleoside following a strategy adapted from literature reports (Scheme 1).[42,43] 2,2′-Anhydro-1-β-D-arabinofuranosyluracil **13** was obtained by reaction of uridine (**12**) with diphenylcarbonate[44] and reacted with the trimethylsilyl ether of neopentyl **15**[45] in the presence of BF_3–Et_2O as the Lewis acid for the activation of the cyclic ether bond (Scheme 1). By using two-fold excess of BF_3–Et_2O and five-fold excess of the trimethylsilyl ether in DMF at 120 °C for 5 days the Un **16** was obtained with an 18% yield after purification. The phosphoramidite building block **18** was obtained by selective 5′-*O*-dimethoxytritylation of the unprotected modified nucleoside **16** with DMTCl in pyridine (compound **17**) followed by reaction with 2-cyanoethyltetraisopropylphosphorodiamidite in the presence of 4,5-dicyanoimidazole with a 50% yield after purification. (Experimental procedures are given *vide infra.*)

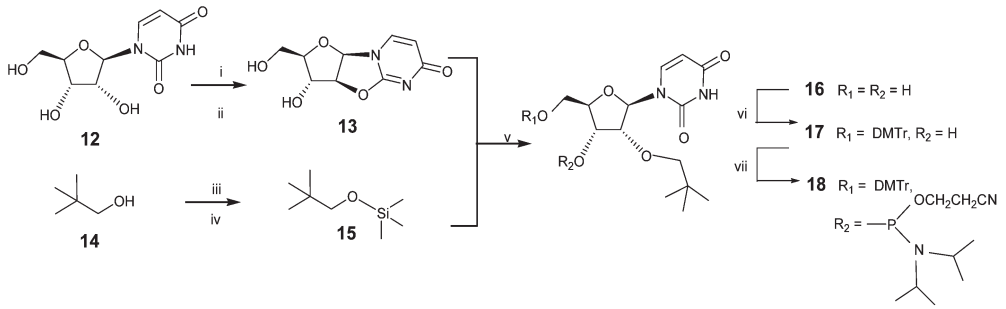

Scheme 1 Synthesis of the modified nucleoside **16** and the phosphoramidite derivative **18**. *Reagents and conditions*: (i) diphenylcarbonate, DMF, 85 °C; (ii) $NaHCO_3$, 120 °C, 4 h; (iii) TMS-Cl, TEA, Et_2O, 0 °C, 30 min; (iv) rt, 72 h; (v) BF_3–Et_2O, DMF, 120 °C, 120 h; (vi) DMTrCl, Py; (vii): 2-cyanoethyltetraisopropylphosphorodiamidite, 4,5-dicyanoimidazole, CH_3CN, CH_2Cl_2.

Synthesis of the oligonucleotides 4–7. The structures of the ONs synthesized are given in Fig. 2. The coupling of 2′-*O*-neopentyldeoxyuridine phosphoramidite **18** was performed using standard procedures. The main change to the typical synthesis was the use of longer coupling times (10 min). The coupling yields were around 97–98% based on a trityl cation assay. The deprotection step was performed using standard conditions (see the Experimental section). After purification by reversed-phase chromatography, the purity of all oligomers described was verified by reversed-phase analysis. Retention times of modified ONs are higher than that of the unmodified ON and increased with the number of Un incorporations (ESI†). These results indicated the presence of more lipophilic compounds. The retention times are also dependent on the position of incorporation of the modified nucleoside. As previously reported with other nucleoside analogues[46] the presence of the modified nucleoside at the 5′-end (ON **4**) induces an increased retention time as compared to its incorporation at the internal position of the sequence (ON **5**). The ON **6** involving three contiguous modified nucleosides is also largely more retained than ON **7** containing also three modified nucleosides but separated by at least two intervening natural nucleosides. The integrity of all ONs was confirmed by MALDI-TOF mass spectrometry (ESI†).

Thermal denaturation studies

The influence of dT replacement (one or three) by 2′-*O*-neopentyldeoxyuridine (Un) on duplex stability was investigated by thermal denaturation studies, followed by absorption spectroscopy, of DNA–DNA and RNA–DNA duplexes obtained by mixing modified ONs **4–7** with 23-mer single-stranded DNA (ON **1**) and RNA (ON **2**) target sequences (X = A) (Fig. 2). For a better understanding of the properties of the new modified nucleoside, the binding properties of ONs **8–11** involving dU incorporations at the same positions were also studied. The purity of ONs **1–3**, **8–11** (from commercial sources) has been verified by reversed-phase chromatography and MALDI-TOF spectrometry before use (data not shown). The melting curves of the DNA–DNA and RNA–DNA duplexes containing the modified ONs **4–7** and the parent duplexes are shown in Fig. 3.

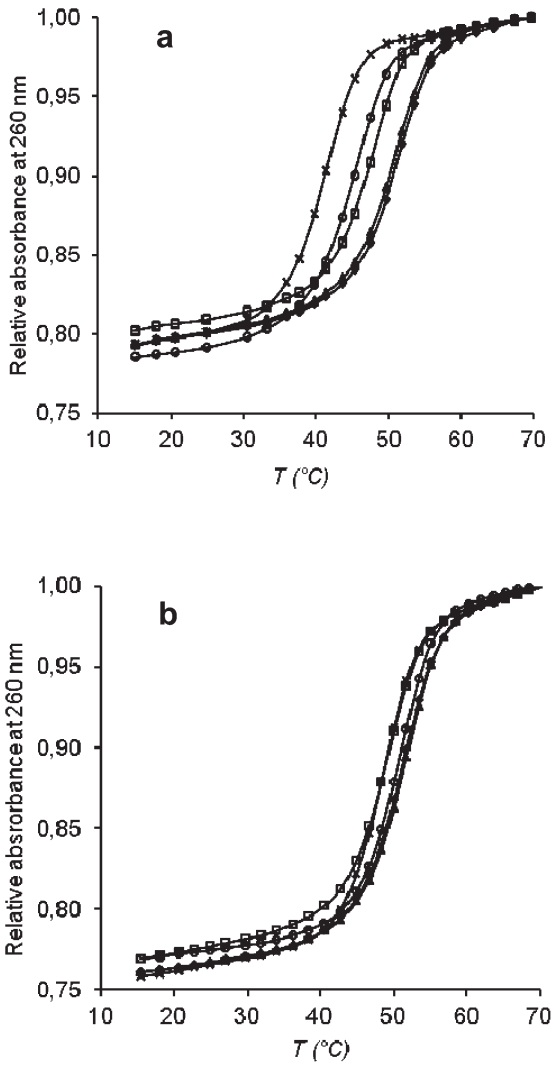

Fig. 3 UV melting curves (260 nm) for DNA–DNA duplexes (a): **1** [5′d-(TAC ACT AAA ACT GGT AAC AAC TC)3′ + ONs **3–7**, and DNA–RNA duplexes (b): **2** [5′r-(UAC ACU AAA ACU GGU AAC AAC UC)3′ + ONs **3** (diamond), **4** (up triangle), **5** (square), **6** (circle) and **7** (cross) in a 10 mM sodium phosphate, pH 7, buffer containing 150 mM NaCl and 1 mM EDTA. Concentrations were 1 μM for each strand. T_m values are reported in Table 1.

Table 1 T_m and thermodynamic parameter data for the duplexes

	1 5′ d-(TAC ACT AAA ACT GGT AAC AAC TC) 3′					**2** 5′ r-(UAC ACU AAA ACU GGU AAC AAC UC)3′				
ONs	T_m [a] (°C)	$\Delta T_{m/mod}$ [a] (°C)	$-\Delta H^0$ (kcal mol^{-1})	$-\Delta S^0$ (eu)	$-\Delta G^0_{37°C}$ [b] (kcal mol^{-1})	T_m [a] (°C)	$\Delta T_{m/mod}$ [a] (°C)	$-\Delta H^0$ (kcal mol^{-1})	$-\Delta S^0$ (eu)	$-\Delta G^0_{37°C}$ [b] (kcal mol^{-1})
3	49.5	—	−132.6	−381.6	−14.2	50.5	—	−137.3	−395.1	−14.7
4	49.4	−0.1	—	—	—	50.6	+0.1	—	—	
5	46.3	−3.2	−122.0	−352.5	−12.7	48.7	−1.8	−127.0	−365.8	−13.6
6	44.1	−1.8	−111.6	−322.9	−11.5	50.4	—	−135.3	−389.2	−14.6
7	40.6	−2.9	−106.7	−311.2	−10.2	47.8	−0.9	−132.9	−385.0	−13.5
8	49.0	−0.5	—	—	—	50.1	−0.4	—	—	—
9	49.0	−0.5	−130.7	−378.1	−13.9	49.7	−0.8	−135.3	−390.3	−14.3
10	47.4	−0.7	−126.2	−364.2	−13.25	48.1	−0.8	−130.0	−375.5	−13.5
11	48.2	−0.4	−126.4	−364.5	−13.35	48.9	−0.5	−130.3	−375.6	−13.8

Experiments were performed in a 10 mM sodium phosphate, pH 7, buffer containing 150 mM NaCl and 1 mM EDTA.[a] Concentrations were 1 μM for each strand and the uncertainty of the T_m value was estimated to be ±1 °C. [b] The thermodynamic data of duplex formation for the modified ONs (**5–7** and **9–11**) and the reference (ON **3**) with the DNA (ON **1**) and RNA (ON **2**) targets were determined from melting curves by the concentration variation method (see the Experimental section). The uncertainty of the $\Delta G^{37°C}$ values can be estimated to be ±10%.

The melting temperatures (T_m) for all duplexes are reported in Table 1. The results are an average of at least two series of independent experiments.

Duplexes with single nucleotide change

Analysis of the data showed different results that were dependent on both the position of the modified nucleoside inside the duplexes (terminal *versus* internal position) and the target considered (DNA *versus* RNA). The presence of the modified nucleoside Un at the 5′-end of the duplex had a less destabilizing effect than its incorporation at the internal position. In the presence of the DNA target (ON **1**), single modifications at the 5′-end of the sequence (ONs **4** and **8**) induced very weak deviations in T_m compared to that of the unmodified duplex (ΔT_m = −0.1 °C for Un and ΔT_m = −0.5 °C for dU). A more pronounced effect was observed (ΔT_m = −3.2 °C) when Un was located at the internal position of the sequence (ONs **5**), while the destabilization induced by the presence of dU (ON **9**) at the same position was weaker (ΔT_m = −0.5 °C). In the presence of the RNA target (ON **2**), the 5′-end modification led to a weak stabilization for Un (ΔT_m = +0.1 °C) and a weak destabilization for dU (ΔT_m = −0.4 °C) while a more pronounced effect was observed for the internal nucleotide substitution (ΔT_m = −1.8 °C for Un and −0.8 °C for dU).

Duplexes with three nucleotide changes

The T_m values were also dependent on both the positions of the modified nucleosides and the target considered (DNA *versus* RNA). In the presence of the DNA target, the incorporation of three Uns in a continuous way (ON **6**) was slightly less destabilizing (ΔT_m = −1.8 °C per modification) than a single incorporation (ON **5**) (ΔT_m = −3.2 °C), while the incorporation of the three Un residues in a discontinuous way (ON **7**) had a much larger destabilizing effect (ΔT_m = −2.9 °C per modification). In the same conditions, the incorporation of three dUs either in a continuous (ON **10**) or in a discontinuous way (ON **11**) had a similar destabilizing effect (ΔT_m = −0.7 °C per modification and ΔT_m = −0.5 °C per modification, respectively). In the presence of the RNA target, the incorporation of the three Uns in a continuous way (ON **6**) led to a T_m value similar to that of the reference (ΔT_m = −0.1 °C) while the incorporation of the three Un residues in a discontinuous way (ON **7**) had a destabilizing effect (ΔT_m = −0.9 °C per modification). In the same conditions, the incorporation of the three dUs either in a row (ON **10**) or in a discontinuous way (ON **11**) had a slight destabilizing effect (ΔT_m = −0.8 °C and −0.5 °C per modification, respectively).

It should be noted that T_m values for the DNA–DNA (ONs **1** + **2**) and DNA–RNA (ONs **1** + **3**) duplexes used as references are very close (ΔT_m = 1 °C). These results are not surprising since T_m values are largely dependent on sequences.[47–49] They are in accordance with the literature data dealing with similar pyrimidine/purine ratios. The incorporation of dU in place of thymidine led to a weak T_m value decrease similar to the literature report.[50] DNA–DNA duplexes containing Un are clearly less stable than the corresponding duplexes involving dU. Conversely, the stability of DNA–RNA duplexes with three Uns in a row is slightly superior to that of the corresponding duplexes involving dU (ΔT_m = +0.8 °C per modification) while the incorporation of Uns in a discontinuous way led to a slight destabilisation (ΔT_m = −0.4 °C per modification). These results show clearly a binding preference for the RNA target that can be tuned by the number and the positions of incorporation of the Un nucleoside.

Mismatch discrimination for DNA–DNA and DNA–RNA duplexes

To determine the base-pairing selectivity in DNA and RNA recognition by Un, ON **5** involving modification at the 11th position was also hybridized with the targets DNA (ON **1**) and RNA (ON **2**) involving cytosine (X = C), guanine (X = G) or thymine (X = T) in the position opposite the modified nucleoside (Table 2). The same experiments were also performed with the ONs **3** and **9**, involving respectively dT and dU, used as references. Observation of the results indicated that in any case the presence of mismatched base-pairs resulted in a dramatic

Table 2 T_m and ΔT_m values for mismatched *versus* matched duplexes

	1 5′d-(TAC ACT AAA **X**CT GGT AAC AAC TC)3′							**2** 5′r-(UAC ACU AAA **X**CU GGU AAC AAC UC)3′						
	X = A	X = T		X = C		X = G		X = A	X = U		X = C		X = G	
ONs	T_m (°C)	T_m (°C)	ΔT_m (°C)	T_m (°C)	ΔT_m (°C)	T_m (°C)	ΔT_m (°C)	T_m (°C)	T_m (°C)	ΔT_m (°C)	T_m (°C)	ΔT_m (°C)	T_m (°C)	ΔT_m (°C)
3	49.5	39.2	−10.3	38.8	−10.7	43.3	−6.2	50.5	41.0	−9.5	40.6	−9.9	47.7	−2.8
5	46.3	39.2	−7.1	37.3	−9.0	41.4	−4.9	48.7	41.2	−7.5	39.0	−9.7	45.7	−3.0
9	49.0	38.6	−10.4	37.3	−11.7	41.9	−7.1	49.7	40.1	−9.6	39.6	−10.1	46.9	−2.8

Left: DNA–DNA duplexes, *Right*: DNA–RNA duplexes. **3**: [5′TTGTTACCAGTTTTAGT3′], **5**: [5′TTGTTACCAG**Un**TTTAGT3′], and **9**: [5′TTGTTACCAG**d**UTTTAGT3′]. Concentrations were 1 μM each strand in a 10 mM sodium phosphate, pH 7, buffer containing 150 mM NaCl and 1 mM EDTA.

decrease of T_m values. However, several differences can be pointed out. When incorporated in DNA–DNA duplexes Un was slightly less efficient than dT and dU at discriminating the mismatches. Conversely, in RNA–DNA duplexes the ΔT_m observed were nearly equivalent in the three series except when rU was the opposite nucleoside. Importantly, the ΔT_m observed for the less destabilizing wobble base pair Un–dG was similar to those obtained for dU–dG and dT–dG. From these experiments, it appears that for the sequence studied ONs involving Un recognize the RNA target with selectivity equivalent to those obtained with the natural dT and the base-modified nucleoside dU.

Thermodynamic data of duplex formation

The thermodynamic data of duplex formation for the modified ONs (**5–7** and **9–11**) and the reference (ON **3**) with both the DNA (ON **1**) and RNA (ON **2**) targets were determined from melting curves by the concentration variation method. The thermodynamic data obtained from $1/T_m$ *versus* log $[C_m]$ plots[51,52] are summarized in Table 1. In the presence of the DNA target, an important decrease of the enthalpy of duplex formation was observed for the three ONs involving Un (**4–7**) as compared to the unmodified ON (**3**) and to the ONs containing dU (**9–11**). This was to some extent counterbalanced by entropy compensation leading to standard enthalpies of duplex formation $\Delta G^{37°C}$ in agreement with the observed thermal stabilities of the different series of duplexes. In the presence of the RNA target, except for ON **5** involving a single Un incorporation, the enthalpy of duplex formation for ONs **6** and **7** involving three Uns was only slightly inferior to that of the reference and slightly superior to those obtained for the corresponding ONs involving the dU nucleosides (**9–10**). For ONs **6** and **7** involving three Uns the changes in entropy terms were also weak as compared to the reference values. The calculated standard enthalpies of DNA–RNA duplex formation $\Delta G^{37°C}$ are in line with the observed thermal stabilities.

CD spectra of modified duplexes

In order to investigate the influence of the incorporation of Un on the duplex structures, we recorded CD spectra of modified ONs involving either one modification (ONs **4**, **5**, **8** and **9**) or three modifications (ONs **6**, **7**, **10** and **11**) in the presence of either their complementary DNA or RNA target sequences (ONs **1** and **2**). The unmodified duplexes (ONs **1** + **3** and **2** + **3**) were used as references. The results are shown in Fig. 4. In the presence of DNA as a complement (Fig. 4a), and compared with the unmodified duplex, the introduction of a single Un (ONs **4** and **5**) resulted in unchanged CD spectra. However, spectra modifications were observed for the duplexes involving three Un nucleosides (ONs **6** and **7**). The presence of three consecutive Uns (ON **6**) resulted in a 30% intensity increase of the positive peak around 275 nm together with a blue shift of about 5 nm (between 270 and 215 nm). The intensity of the negative peak at 245 nm was also slightly reduced. The CD spectra of the DNA–DNA duplex involving the three Uns at non-consecutive positions was also changed as compared to that of the unmodified duplex. A blue shift was also observed as well as a reduced negative peak at 245 nm slightly more pronounced than for the duplex involving the contiguous Uns. These changes reflect differences in the duplex structures due to the presence of the neopentyl group at the 2′-position of the 2′-deoxyribose. The CD spectra of the duplexes involving dU are identical to that of the unmodified DNA–DNA duplex (Fig. 4c).

As observed for the DNA–DNA duplexes the presence of a single Un in the DNA–RNA duplexes did not result in modifications in the CD spectra (Fig. 4b). But changes were observed for the duplexes involving three Uns. Once again, a slight blue shift and also intensity changes were observed for both duplexes. A small intensity increase at 260 nm and an important decrease at 220 nm were observed for the duplex with three contiguous Uns, and only a very weak intensity decrease at 270 nm for the duplex with three non-contiguous Uns. The CD spectra of the DNA–RNA duplexes containing dU were identical to that of the DNA–RNA unmodified duplex except in the case of the presence of three contiguous dUs for which a small blue shift was observed between 255 and 215 nm (Fig. 4d). Comparison with the data obtained for the DNA–RNA duplexes involving dU incorporations in the same positions allowed the conclusion that the observed weak spectra modifications reflect small structural changes of the duplexes that are mainly due to the presence of the neopentyl group.

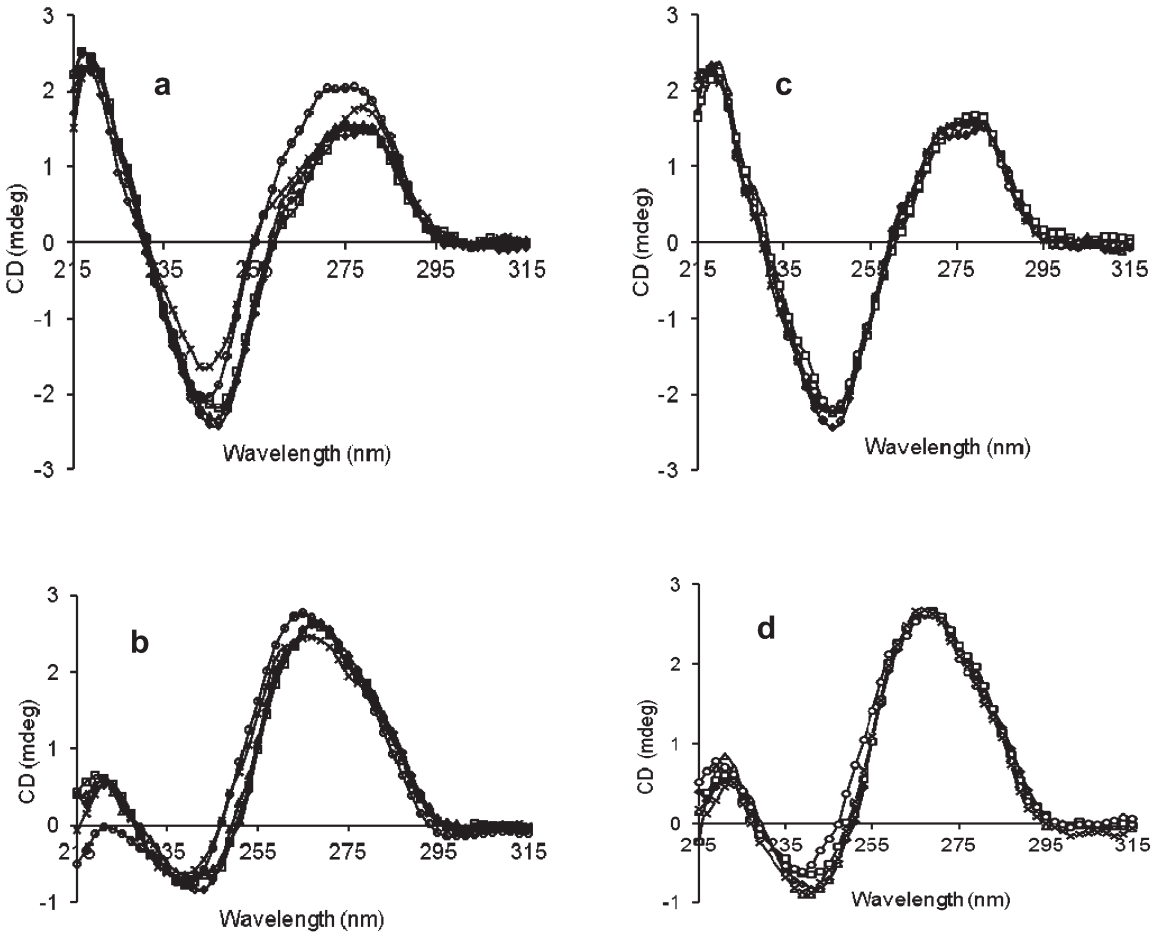

Fig. 4 CD spectra of the unmodified and modified duplexes [4 μM solutions (each strand) in a 10 mM sodium phosphate, pH 7, buffer containing 150 mM NaCl and 1 mM EDTA] were recorded at 10 °C between λ = 215 and 315 nm. (a): DNA target **1** and ONs **3** (diamond), **4** (up triangle), **5** (square), **6** (circle) and **7** (cross); (b): RNA target **2** and ONs **3** (diamond), **4** (up triangle), **5** (square), **6** (circle) and **7** (cross); (c): DNA target **1** and ONs **3** (diamond), **8** (up triangle), **9** (square), **10** (circle) and **11** (cross); (d): RNA target **2** and ONs **3** (diamond), **8** (up triangle), **9** (square), **10** (circle) and **11** (cross).

Although weak spectra changes were observed for the duplexes involving three Uns, their general shapes were similar to those of the B-type DNA–DNA and A/B type RNA–DNA unmodified duplexes.

Molecular dynamic simulations

In order to correlate the thermal and thermodynamics properties of the different series of duplexes with structures on a more detailed level, we performed molecular dynamic simulations of 5 ns on the DNA–DNA and DNA–RNA duplexes involving a single internal incorporation of Un as well as those involving three Un incorporations. The structures of the corresponding duplexes involving dU were also investigated. Simulations of the unmodified DNA–DNA and DNA–RNA duplexes were used as references (see the Experimental section for conditions).

DNA–DNA duplexes

The six DNA–DNA duplexes containing Un and dU modified nucleosides showed a stable helical structure during the 5 ns of simulation without any base-pair disruption and showed an average value of their calculated curvature comparable to the reference. The RMSD times-series were quickly stabilized around values from 2.4 Å to 3.4 Å. For the three duplexes containing the modified nucleoside Un, we observed that the neopentyl group remained stable and localized in the minor groove. The positioning of the neopentyl group is shown in Fig. 5a. The variations of the sugar pucker conformation of each residue during the simulation in the form of a heat map for the DNA–DNA duplex involving a single Un are shown in ESI (Fig. 6a†). We observed that all residues conserved a C2′-*endo* sugar pucker conformation, B-helix type, during the entire simulation time except the Un residue that adopted a C2′-*exo* sugar pucker conformation, close to an A-helix type. The same result was observed for the DNA–DNA duplexes containing three Uns where all residues adopted a C2′-*endo* sugar pucker conformation (B-helix) except the modified nucleoside Uns that adopted a C2′-*exo* sugar pucker conformation (close to an A-helix) (data not shown). For the three simulations involving dU nucleosides, all the residues adopt a C2′-*endo* sugar pucker conformation and the heat maps obtained cannot be distinguished from the reference (data not shown).

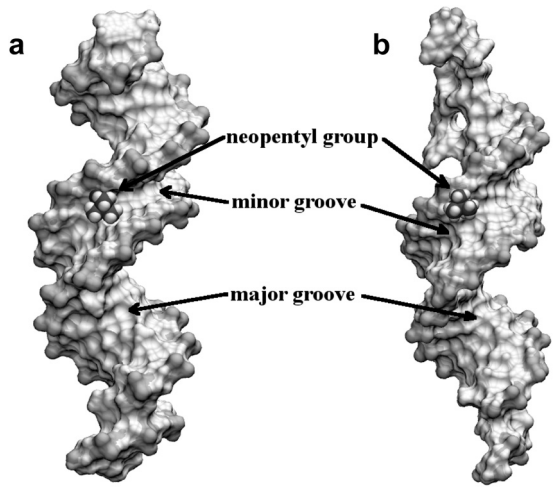

Fig. 5 Structure visualization of duplexes: DNA–DNA (a) and DNA–RNA (b), containing a single modified nucleoside Un. Standard nucleoside atoms are represented as surface and neopentyl group atoms as van der Walls spheres.

We also studied the evolution of major and minor groove width of each duplex during the simulation. The results obtained for the minor groove width measured on unmodified DNA–DNA duplex are shown in Fig. 7a (ESI†). A narrowing of the minor groove width (around 8–10 Å in blue, instead of 12–15 Å in green) due to the presence of an A-tract in the target sequence was observed. This phenomenon has been largely described in the literature.[53–57] The incorporation of a single Un nucleotide in the T-tract sequence also caused a narrowing of the minor groove (data not shown). However, the presence of three Un nucleosides, contiguous or not, prevented the narrowing of the minor groove probably due to the presence of the neopentyl groups localized in the minor groove. Fig. 7b in ESI† shows the heat map for the DNA–DNA duplex involving three non-contiguous Uns. Finally, we estimated the average solvent-accessible surface area (SASA) of the neopentyl residues for the three duplexes containing the modified nucleoside Un in order to correlate their exposure to the solvent with their number and positioning in the sequence. We observed a lower neopentyl exposure to the solvent (~240 $Å^2$) for a single and three contiguous modifications. In the first case, the low exposure was probably due to the groove narrowness that tends to bury the neopentyl group while in the second case, the decrease of exposure was due to the proximity of the three neopentyl groups. On the contrary, the introduction of three non-contiguous Un nucleosides increased the solvent exposure of the neopentyl groups (~260 $Å^2$). This is consistent with the fact that the presence of a second Un nucleoside within the T tract prevents the narrowing of the minor groove.

RNA–DNA duplexes

We still observed that the six DNA–RNA duplexes containing modifications remained stable with a conserved helical structure during the 5 ns of simulation without any base-pair disruption or significant curvature. The RMSD times-series were stabilized around higher values than the DNA–DNA duplexes, from 2.7 Å to 5.0 Å, which was probably caused by a longer adaptation time for the DNA–RNA hybridization. However, for the three duplexes containing the modified nucleoside Un, the neopentyl group was stable and well-localized in the minor groove. The positioning of the neopentyl group is shown in Fig. 5b. Heat maps of the sugar pucker conformation variations of paired residues during the simulation showed two distinct areas. The RNA strand showed the characteristic sugar pucker conformations of an A-helix whereas those obtained for the DNA strand were characteristic of a B-helix. As for DNA–DNA duplexes, the Un modifications inserted on the DNA strand adopted the characteristic sugar pucker conformations of an A-helix without disturbing their neighboring sugar pucker conformations. The heat map of the sugar pucker conformation variations of paired residues for the DNA–RNA duplex containing a single modified nucleoside Un is shown in Fig. 6b in ESI.† The A-tract influence on the minor groove width is less visible on the DNA–RNA hybrids than on the DNA–DNA hybrids (Fig. 7 in ESI†). A slight effect is however still discernible on the minor groove of the unmodified DNA–RNA duplex (Fig. 7c†) and the modified DNA–RNA duplex involving a single Un that is not observed for the DNA–RNA duplexes involving three Un modifications, contiguous or not. The heat map for the DNA–RNA duplex involving three non-contiguous Uns is shown in Fig. 7d in ESI.† Finally, the solvent exposure of the Un nucleosides was globally higher in DNA–RNA duplexes than in DNA–DNA duplexes, which could be explained by the widening of the A-tract minor groove in DNA–RNA duplexes compared to DNA–DNA duplexes. However, we always observed a decrease of solvent exposure for the three contiguous Uns. So we noticed a slight increase of the solvent exposure dependent on the number and positioning of the Un nucleosides. The most reduced solvent exposure occurred with the insertion of three contiguous Uns (~255 $Å^2$) followed by the insertion of one Un modification (~270 $Å^2$) which is comparable with the insertion in the A-tract of three discontinuous Un modifications (~275 $Å^2$).

The results of the melting studies and CD experiments are consistent with those of the molecular simulation studies indicating that either a single or three neopentyl groups, in different arrangements, were able to be accommodated in the minor groove of both the DNA–DNA and RNA–DNA duplexes. However, an important difference was observed between the structures involving dU and Un modified nucleosides in the simulations. While a C2′-*endo* sugar pucker was conserved in all the dU residues, all the Un residues adopted a C2′-*exo* sugar pucker conformation, close to an A-helix type. The results of the melting studies indicated a binding preference of the ONs **5**, **6** and **7**, involving Un residues, for the RNA over the DNA complement, whatever the number and positions of modifications. The selectivity of Un base-pairing in RNA–DNA duplexes was equivalent to those of dT and dU and slightly weaker in the presence of the DNA targets. Another observation concerns the non-additive effect of three Un incorporations. While a single Un incorporation at the internal

position of the sequence (ON **5**) had a destabilizing effect (relative to dU) (ΔT_m = −1 °C per modification for the RNA–DNA duplex and ΔT_m = −2.7 °C per modification for the DNA–DNA duplex), the presence of three consecutive Uns (ON **6**) stabilized the RNA–DNA duplex (ΔT_m = +0.8 °C per modification) and destabilized the DNA–DNA duplex (ΔT_m = −1.1 °C per modification). When the three Un insertions were spaced by at least two natural 2′-deoxynucleosides both the RNA–DNA and DNA–DNA duplexes were destabilized (ΔT_m = −0.4 °C per modification and ΔT_m = −2.5 °C per modification, respectively). Although a single Un incorporation in both the DNA–DNA and RNA–DNA duplexes was destabilizing, their CD spectra were indistinguishable from those reported for the unmodified duplexes and those containing dU at the same position. Only a small blue shift at 275 nm and reduced intensity at 220 nm were observed for the CD spectra of the most stable RNA–DNA duplex involving three contiguous Uns. The most important changes in CD spectra were observed for the DNA–DNA duplexes involving three non-consecutive Uns (corresponding to the less stable duplex). They consisted of a slight blue shift associated with 30% increase at 275 nm when Uns were consecutive and a reduced negative peak at 245 nm in the presence of non-consecutive Uns.

On the basis of these results and the literature reports on modified oligonucleotides involving different series of 2′-modified nucleosides several observations can be made and hypotheses suggested to explain the different binding abilities observed for our modified ONs involving the modified 2′-*O*-neopentyldeoxyuridine. Different classes of 2′-modified nucleosides have been incorporated into ONs.[6,16,18,24,30,37,40,58–66] Among them, those involving *O*-methyl,[34,40] *O*-2′-*O*-methoxyethyl,[31,36] 2′-*O*-[2-(methyl-amino)-2-oxoethyl],[36] 2′-*O*-(3-aminopropyl),[60,61] 2′-*O*-[2-(guanidinium)ethyl][62] and 2′-fluor[18,24,58,59] substituents have been reported to improve the biophysical properties of ONs. A specific mention must be made of the 2′-*O*,4′-C-methylene bicyclonucleosides[6,25,26,28,64,65] being among the most useful modified nucleosides to date exhibiting unique binding properties on the basis of their use in a great variety of applications. The improved binding affinities of these different classes of modified ONs have been reported to rely mainly on their tendency to adopt the 2′-*exo* pucker conformation. The binding affinities of the 2′-modified ONs are also influenced by other different parameters: the size of the 2′-*O*-substituent, the number and positions of the modified nucleosides, the sequence effect, the hydration changes in the minor groove and potential additional interactions between heteroatoms present in the substituents and the ON backbone.

More specifically, comparison of our results with the literature reports on ONs involving a few nucleosides modified at the 2′-position with aliphatic alkyl groups in a background of 2′-deoxynucleosides showed similar behaviors.[16,35] These modified ONs were able to form DNA–DNA and RNA–DNA hybrids with stabilities dependent on the size and structure of the pendent groups at the 2′-position. The thermal stability of the complexes was reduced as the length of the 2′-*O*-alkyl chain increased. It has also been shown that the binding affinities of these modified ONs were largely sequence dependent and also dependent on the number and positions of the modified nucleosides inside the sequence. So the comparison of the ΔT_m per modification cannot be quantitative. However, it has been reported that substitutions smaller than 2′-*O*-propyl stabilized the RNA–DNA duplexes. The literature report on modified ONs involving 2′-*O*-modified adenosines indicated that the incorporation of five 2′-*O*-alkylated adenosines involving methyl, ethyl, propyl, butyl or pentyl groups in purine-rich ONs did not change the CD spectra of the RNA–DNA duplexes compared to the parent while a bulkier group induced important changes.[35] In addition, similarly to our finding, the effects of several incorporations were not additives. It has been reported that for almost every modification (including *O*-ethyl) the ΔT_m per modification was negative in ONs that contained a single substitution and three consecutive 2′-substitutions were less destabilizing (or more stabilizing) than isolated substitutions spaced by unmodified deoxynucleosides. As observed with our modified ONs, 2′-*O*-substitutions on adenosine have been reported to induce a binding preference for their RNA over DNA complements.

The RNA binding preference of ONs involving Un nucleosides is likely due to the tendency of the 2′-modified nucleosides to adopt a 2′-*exo* geometry inconsistent with B-form DNA–DNA geometry. Furthermore, the presence of the neopentyl groups could induce more perturbations of the hydration in the minor groove of the DNA–DNA duplex than in the minor groove of the RNA–DNA duplex. Concerning the variations in ΔT_m per modification, although the same trend was observed in the presence of both the DNA and the RNA targets, several observations can be made. A single incorporation of Un (ON **5**) was performed at the end of a tract of four consecutive A–T base-pairs. It is known that this structure facilitates formation of a water spine in the minor groove of the B-DNA stabilizing the duplex. Furthermore the minor groove width of the unmodified dA–dT tract was reduced.[53–57] The results of molecular simulation studies indicated that the incorporation of a single Un nucleotide in the T-tract sequence also caused a narrowing of the minor groove. However, the presence of three Un nucleosides, contiguous or not, prevented the contraction of the minor groove. It should be noted that in ON **7** involving three non-contiguous Uns, both of them were located in the T-tract and separated by two natural 2′-deoxynucleosides. In the RNA–DNA duplexes the A-tract influence on the minor groove width was still present but less visible than on the DNA–DNA hybrids. In addition, the decrease of solvent exposure observed when three Uns were consecutive suggested that interactions between them were possible on the surface of the minor groove which could also be a source of additional stabilization.

We have reported the ability of modified ONs, involving either one or three modified 2′-*O*-neopentyluridines, to hybridize preferentially with their RNA target sequences with a stability increase of +0.8 °C per modification when the modified

nucleosides are consecutive. This affinity increase is nearly similar to that observed for fully modified 2′-*O*-methyl and 2′-*O*-propyl ONs.[36] It is likely that the incorporation of 2′-*O*-neopentyluridines in different numbers and arrangements in other sequences could lead to slightly different binding properties. However, the incorporation of a greater number of 2′-*O*-neopentyluridines introducing more A-character for the duplex formed with the RNA complement could contribute to an increased stabilization of the duplex as previously reported for ONs involving other 2′-*O*-alkyled nucleosides.[36] In addition, Un nucleosides could be used in association with other modified nucleosides able to adopt a 2′-*exo* geometry to obtain a modulation of the binding affinity of modified ONs.

Conclusion

A 2′-deoxyuridine analogue involving a neopentyl group at the 2′-position Un was synthetized and incorporated into a series of 17-mer ONs. The modified ONs involved either one (at the 5′-end or the internal position) or three (either in a contiguous fashion or separated by at least two natural nucleosides) modified Un nucleosides. The corresponding series of 17-mer ONs involving dU at the same positions was also used for comparison. The pairing ability of these two series of ONs with their DNA and RNA complements was investigated by thermal denaturation and circular dichroism measurements. The results showed clearly the ability of all modified ONs to specifically bind their DNA and RNA targets with the formation of duplex structures similar to those of the B-type DNA–DNA and A–B type RNA–DNA references. Small changes in the CD spectra were observed only for the duplexes containing three Un nucleosides. Different duplex stabilities were observed. The presence of Un at the terminal position of the duplexes had no effect on their stability. However, a single incorporation at the internal position had a destabilizing effect in the presence of both the DNA and RNA complements (ΔT_m = −2.7 °C and ΔT_m = −1 °C, respectively relative to the corresponding duplexes containing dU). The presence of three Uns led to different duplex stability changes dependent on both their arrangements and the target considered. In all cases, the presence of three Uns in DNA–DNA duplexes had a destabilizing effect. However, the presence of three contiguous Uns had a less important effect (ΔT_m = −1.1 °C per modification relative to dU) as compared to their incorporation in a non-contiguous way (ΔT_m = −2.5 °C per modification relative to dU). Three consecutive Un incorporations led to the RNA–DNA duplex with a stability slightly superior to that of the RNA–DNA duplex containing dU–rA pairs (ΔT_m = +0.8 °C per modification) while a slight destabilization was observed (ΔT_m = −0.4 °C per modification relative to dU) when the three Uns were inserted in a non-contiguous fashion. This trend was confirmed by the results of the thermodynamic investigations. To rationalize these differences in stability, the behaviour of the modified nucleosides Un and dU in the different duplexes was evaluated by molecular dynamic simulations. The results showed for all duplexes stable helical structures during the 5 ns of simulation, similar to the reference, without any base-pair disruption. For the duplexes containing the modified nucleoside Un, the neopentyl group remained stable and localized in the minor groove. However, an important difference was observed between the structures involving dU and Un modified nucleosides. While in the modified ONs containing the dU modified nucleosides all the residues adopted a C2′-*endo* sugar pucker conformation, in the modified ONs involving the new modified Un nucleoside all residues conserved a C2′-*endo* sugar pucker conformation, except the Un residues which adopted a C2′-*exo* sugar pucker conformation, close to an A-helix type. The differences in stability observed for the DNA–DNA and RNA–DNA duplexes, involving three Uns in different arrangements, can be explained by the sequence context, the local minor structure changes as well as by the hydration changes. On the basis of these results, Un represents an interesting dU analogue that could be used for tuning the hybridization properties of ONs and due to this is worthy of further exploration for applications in oligonucleotide therapeutic based strategies.

Experimental

General methods

All solvents used were of the highest purity and did not contain more than 10 ppm H_2O. All chemicals were used as obtained unless otherwise stated. Analytical TLC was performed on pre-coated alumina plates (Merck silica gel 60F 254, ref. 5554), and preparative TLC on glass-backed silica plates (60F 254, ref. 5717). For flash chromatography, Merck silica gel 60 (70–230 mesh, ref. 7734) was used. Compounds were directly visualized on the plates by UV-shadowing. ODN syntheses were performed on an Expedite Nucleic Acid Synthesis system 8909 from PerSeptive Biosystems. Reversed-phase chromatography was performed on a 600E (System Controller) equipped with a photodiode array detector (Waters 990) using a Lichrospher 100 RP 18 (5 mm) column (125 mm × 0.4 mm) from Merck with a linear gradient of CH_3CN in 0.1 M aqueous triethylammonium acetate, pH 7, with a flow rate of 1 cm^3 min^{-1}. Oligonucleotides containing dU were from Eurogentec and RNA sequence from Biomers. ^1H NMR, ^{13}C NMR and ^{31}P NMR were recorded at 400 MHz, 100 MHz and 162 MHz, respectively. ^1H chemical shifts are reported in ppm relative to either residual solvent peak DMSO (2.54 ppm) or Me_4Si. ^{31}P chemical shifts were referenced to H_3PO_4 (external reference). The following abbreviations are used for the proton spectra multiplicities: s: singlet, d: doublet, t: triplet, q: quartet, qt: quintuplet, m: multiplet, br: broad, dd: doublet of doublet, dt: doublet of triplet. Coupling constants (*J*) are reported in Hz. Absorption spectra were recorded with an Uvikon 860 spectrophotometer. The molar extinction coefficient of the modified nucleosides was considered to be equivalent to that of the 2′-deoxyuridine. Consequently, the molar

extinction coefficients of ONs were determined according to the literature.[67]

Synthesis

2,2′-Anhydrouridine 13.[44] To a suspension of uridine **12** (40 g, 0.16 mol) into dry DMF (44 cm^3) was added diphenyl carbonate (38.6 g, 0.18 mol) under argon at room temperature. The mixture was stirred at 85 °C until the slurry became clear, then sodium hydrogen carbonate (0.21 g, 2.50 mmol) was added. After stirring at 120 °C for 4 hours, the reaction was diluted with MeOH (60 cm^3) and then filtered through a bunker funnel and the solid washed with MeOH. The solid was re-suspended into MeOH (60 cm^3) and stirred for 30 min at room temperature. The suspension was again filtered to yield **13** (27.43 g, 0.12 mol, 74%) as white solid. R_{f13} 0.12 ($CHCl_3$–MeOH, 95 : 5, v/v). δ_H (400 MHz, DMSO-d_6), 3.18 [1H, m, H–C(5′)]; 3.28 [1H, m, H–C(5′)]; 4.06 [1H, dt, J = 0.8, 4.8 Hz, H–C(4′)]; 4.38 [1H, s, H–C(3′)]; 4.97 [1H, s, HO–C(5′)]; 5.19 [1H, d, J = 6.0 Hz, H–C(2′)]; 5.83 [1H, d, J = 7.6 Hz, H–C(5)]; 5.88 [1H, d, J = 7.2 Hz, HO–C(3′)]; 6.30 [1H, d, J = 5.6 Hz, H–C(1′)]; 7.83 [1H, d, J = 8.4 Hz, H–C(6)]. δ_C (100 MHz, DMSO-d_6), 60.7 [1t, C(5′)]; 74.6 [1d, C(3′)]; 88.6 [1d, C(2′)]; 89.1 [1d, C(4′)]; 89.9 [1d, C(1′)]; 108.5 [1d, C(5)]; 136.7 [1d, C(6)]; 159.7 [1s, C(4)]; 171.1 [1s, C(2)]. HRMS (ESI^+-TOF): m/z, found 227.0664 ($[M + H]^+$, $C_9H_{11}N_2O_5$ calc. 227.0662).

1-Trimethylsilyloxy-2,2-dimethylpropane 15.[45] To a solution of neopentyl alcohol **14** (20 g, 0.23 mol) into dry Et_2O (150 cm^3) was added dropwise a solution of TMS-Cl (35 cm^3, 0.28 mol) and TEA (39 cm^3, 0.28 mol) into dry Et_2O (50 cm^3) over 30 minutes at 0 °C. The reaction was stirred for 3 days at room temperature and then filtered. The precipitate was washed with Et_2O then the filtrate was concentrated under reduced pressure. The crude product was distilled under atmospheric pressure to yield **15** (25.31 g, 0.16 mol, 69%) as a colourless liquid. bp 130 °C–760 mmHg (lit.,[45] bp 122 °C–734 mmHg). δ_H (400 MHz, $CDCl_3$), 0.09 [9H, s, –Si(CH_3)$_3$]; 0.86 [9H, s, –C(CH_3)$_3$]; 3.20 (2H, s, CH_2). δ_C (100 MHz, $CDCl_3$), −0.5 [q, Si(CH_3)$_3$]; 26.6 [q, –C(CH_3)$_3$]; 32.6 [s, –C(CH_3)$_3$]; 72.8 (d, CH_2). MS characterization has been unsuccessful.

2′-*O*-Neopentyluridine 16. To a suspension of 2,2′-anhydrouridine **13** (3.50 g, 15.5 mmol) and 1-trimethylsilyloxy-2,2-dimethylpropane **15** (12.4 cm^3, 77.3 mmol) into 31 cm^3 of dry DMF was added BF_3–Et_2O (4.8 cm^3, 38.8 mmol) under argon. The mixture was stirred at 120 °C for 5 days and then cooled down at room temperature. The precipitate was filtered through a bunker funnel and washed with EtOAc. The filtrate was diluted with EtOAc (250 cm^3) and washed with brine (4 × 150 cm^3). The organic phase was dried over Na_2SO_4, filtered and concentrated to dryness under reduced pressure. The crude product was purified by silica gel chromatography (eluent: CH_2Cl_2–MeOH 100 : 0, v/v to CH_2Cl_2–MeOH 95 : 5, v/v) to yield **16** (0.88 g, 2.8 mmol, 18%) as a white solid. R_{f16} 0.40 ($CHCl_3$–MeOH, 85 : 15, v/v). δ_H (400 MHz, DMSO-d_6), 0.85 [9H, s, –CH_2C(CH_3)$_3$]; 3.12 [1H, d, J = 8.8 Hz, –CH_2C(CH_3)$_3$]; 3.30 [1H, d, J = 8.8 Hz, –CH_2C(CH_3)$_3$]; 3.56 [1H, m, H–C(5′)]; 3.66 [1H, m, H–C(5′)]; 3.81 [1H, dt, J = 4.8 Hz, H–C(2′)]; 3.88 [1H, m, H–C(4′)]; 4.07 [1H, q, J = 5.2 Hz, H–C(3′)]; 4.97 [1H, d, J = 6 Hz, HO–C(3′)]; 5.11 [1H, t, J = 4.8 Hz, HO–C(5′)]; 5.63 [1H, d, J = 8.0 Hz, H–C(5)]; 5.83 [1H, d, J = 4.8 Hz, H–C(1′)]; 7.83 [d, J = 8.0 Hz, H–C(6)]; 11.30 (1H, s, –NH). δ_C (100 MHz, DMSO-d_6), 26.2 [1q, –CH_2C(CH_3)$_3$]; 31.9 [1s, –$CH_2$$C$($CH_3$)$_3$]; 60.3 [1t, C(5′)]; 68.3 [1d, C(3′)]; 79.8 [1t, –$C$$H_2$C($CH_3$)$_3$]; 82.4 [1d, C(2′)]; 84.9 [1d, C(4′)]; 86.1 [1d, C(1′)]; 101.6 [1d, C(5)]; 140.3 [1d, C(6)]; 150.3 [1s, C(2)), 163.0 (1s, C(4)]. HRMS (ESI^+-TOF): m/z, found 337.1360 ($[M + Na]^+$, $C_{14}H_{22}N_2O_6Na^+$ calc. 337.1376).

5′-*O*-Dimethoxytrityl-2′-*O*-neopentyluridine 17. To a solution of 2′-*O*-neopentyluridine **16** (1.59 g, 5.05 mmol) into dry pyridine (40 cm^3) was added dropwise at 0 °C a solution of dimethoxytrityl chloride (2.05 g, 6.06 mmol) into dry pyridine (10 cm^3) over 1 hour. After stirring for 5 hours at room temperature, the reaction was quenched with MeOH (0.5 cm^3). The reaction was again stirred for 30 minutes and then diluted with CH_2Cl_2 (100 cm^3). The mixture was washed successively with cold water (3 × 50 cm^3), cold 5% aq. $NaHCO_3$ (2 × 50 cm^3) and cold brine (50 cm^3). The organic phase was dried over Na_2SO_4 and concentrated to dryness under reduced pressure. The residue was co-evaporated with toluene (2 × 25 cm^3) and purified by silica gel chromatography (the column was packed with eluent containing 5% TEA to prevent detritylation, eluent: hexane–EtOAc–TEA, 80 : 19 : 1 v/v/v to hexane–EtOAc–TEA, 50 : 49 : 1, v/v/v) to yield **17** (1.78 g, 2.88 mmol, 57%) as a white foam. R_{f17} = 0.59 (CH_2Cl_2–MeOH, 9 : 1, v/v). δ_H (400 MHz, $CDCl_3$), 0.95 [9H, s, –CH_2C(CH_3)$_3$]; 2.62 [1H, d, J = 9.6 Hz, HO–C(3′)]; 3.29 [1H, d, J = 9.2 Hz, –OCH_2C(CH_3)$_3$]; 3.53 [1H, dd, J = 2.8, 11.2 Hz, H–C(5′)]; 3.58 [1H, dd, J = 2.0, 11.2 Hz, H–C(5′)]; 3.66 [1H, d, J = 9.2 Hz, –OCH_2C(CH_3)$_3$]; 3.79, 3.80 (6H, 2s,–OCH_3); 3.87 [1H, d, J = 5.2 Hz, H–C(2′)]; 4.02 [1H, m, H–C(4′)]; 4.47 [1H, dt, J = 5.2, 8.8 Hz, H–C(3′)]; 5.28 [1H, d, J = 8.0 Hz, H–C(5)]; 5.93 [1H, s, H–C(1′)]; 6.83–6.86 (4H, m, arom. H); 7.22–7.32 (7H, m, arom. H); 7.38–7.41 (2H, m, arom. H); 8.04 [1H, d, J = 8.4 Hz, H–C(6)]; 9.30 (1H, br s, –NH). δ_C (100 MHz, $CDCl_3$), 26.5 [q, –C(CH_3)$_3$]; 32.2 [s, –C(CH_3)$_3$]; 55.2 (q, –OCH_3); 61.1 [t, –O$C$$H_2$C($CH_3$)$_3$]; 68.4, 80.9, 82.7, 83.3, 87.1 [4d, 1t, C(1′), C(2′), C(3′), C(4′), C(5′)]; 87.4 [s, –C(Ar)$_3$]; 101.9 [d, C(5)]; 113.3 (d, arom. CH), 127.1, 127.9, 128.1, 130.1, 130.2 (5d, arom. CH), 135.0, 135.3 (2s, arom. Cq), 140.0 [d, C(6)]; 144.3 (s, arom. Cq), 150.0 [s, C(2)]; 158.6, 158.7 (2s, arom. Cq); 163.4 [s, C(4)]. HRMS (ESI^+-TOF): m/z, found 639.2675 ($[M + Na]^+$, calc. 639.2682).

5′-*O*-Dimethoxytrityl-3′-*O*-(2-cyanoethyl-*N*,*N*′-diisopropylphosphoramidite)-2′-*O*-neopentyluridine 18. To a mixture of 5′-*O*-dimethoxytrityl-2′-*O*-neopentyluridine **17** (2.10 g, 3.41 mmol) and 4,5-dicyanoimidazole (0.27 g, 2.28 mmol, 0.25 M in CH_3CN) into dry CH_2Cl_2 (43 cm^3) was added dropwise 2-cyanoethyl-*N*,*N*,*N*′,*N*′-tetraisopropylphosphorodiamidite (1.6 cm^3, 5.12 mmol) over 10 minutes under argon. The reaction was stirred for 1 hour at room temperature and then diluted with CH_2Cl_2 (100 cm^3). The mixture was washed with cold 5% aq. $NaHCO_3$ (2 × 50 cm^3) and cold brine (50 cm^3). The organic phase was dried over Na_2SO_4 and evaporated to dryness under reduced pressure. The residue was purified by silica gel chromatography (the column was packed with eluent containing 5%

TEA to prevent detritylation, eluent: CH_2Cl_2–TEA (99 : 1, v/v) to CH_2Cl_2–EtOAc–TEA, 70 : 29 : 1, v/v/v) to yield **18** (1.81 g, 2.22 mmol, 65%) as a white foam. R_{f18} = 0.35, 0.42 (CH_2Cl_2–EtOAc, 8 : 2, v/v). δ_H (400 MHz, $CDCl_3$), 0.91, 0.93 [9H, 2s, $-CH_2C(CH_3)_3$]; 1.04–1.30 [6H, m, 3H, $-CH(CH_3)_2$]; 2.43 (1H, t, J = 6.0 Hz, $-OCH_2CH_2CN$); 2.61 (1H, t, J = 6.0 Hz, $-OCH_2CH_2CN$); 3.32–3.99 [7H, m, $-OCH_2C(CH_3)_3$, $-CH_2(5')$, $-OCH_2CH_2CN$, $-NCH(CH_3)_2$], 3.78, 3.79, 3.80, 3.81 (6H, 4s, $-OCH_3$); 3.97, 3.98 [1H, 2m, H–C(2′)], 4.23, 4.28 [1H, 2m, H–C(4′)], 4.39–4.56 [1H, 2m, H–C(3′)], 5.20, 5.22 [1H, 2d, J = 8.2 Hz, H–C(5)]; 5.91, 5.94 [1H, 2d, J = 2 Hz, H–C(1′)]; 6.82–6.86 (4H, m, arom. H); 7.33–7.86 (7H, m, arom. H); 7.38–7.43 (2H, m, arom. H); 8.01, 8.08 [1H, 2d, J = 8 Hz, H–C(6)]; 8.67 (br s, 1H, –NH). δ_C (100 MHz, $CDCl_3$), 20.2, 20.4 (2dt, J = 6.9 Hz, $-OCH_2CH_2CN$); 24.5–24.8 [m q, $-CH(CH_3)_2$]; 26.5, 26.6 [2q, $-CH_2C(CH_3)_3$]; 32.1, 32.2 [2s, $-CH_2C(CH_3)_3$]; 43.1, 43.2 [2dd, J = 12.7 Hz, $-CH(CH_3)_2$]; 55.2, 55.3 (2q, $-OCH_3$); 57.8, 58.1 (2dt, J = 18.3 Hz, $-OCH_2CH_2CN$); 60.7, 61.1 [2t, $-CH_2C(CH_3)_3$]; 69.9–87.1 [1t, 4d, C(1′), C(2′), C(3′), C(4′), C(5′)]; 87.9, 88.1 [2s, $-C(Ar)_3$]; 101.7, 101.8 [2d, C(5)]; 113.2 (d, arom. CH), 117.4, 117.5 (2s, –CN), 127.1, 127.9, 128.0, 128.2, 128.3, 130.3 (6 d, arom. CH); 134.9, 135.1, 135.2, 135.3 (4s, arom. Cq); 140.1, 140.2 [2d, C(6)]; 144.2, 144.3 (2s, arom. Cq), 149.9, 150.0 [2s, C(2)]; 158.6, 158.7 (2s, arom. Cq); 163.2, 163.3 [2s, C(4)]. ^{31}P NMR (162 MHz, $CDCl_3$), δ = 149.6, 149.8. $C_{44}H_{57}N_4O_9P$ (816.92). HRMS (ESI^+-TOF): m/z, found 839.3773 ($[M + Na]^+$, $C_{44}H_{57}N_4O_9NaP^+$, calc. 839.3761).

Oligonucleotide synthesis, purification and characterization. All ONs were prepared from modified nucleoside phosphoramidite **18** and commercially available dA, dC, dG, and dT phosphoramidites (Biosolve) and deoxynucleoside-CPG (1 μmol, Glen Research) on an *Expedite Nucleic Acid* automated synthesizer by standard solid-phase phosphoramidite chemistry except for the modified phosphoramidite **18**. The coupling time increased to 10 min. Tetrazole (0.45 M in MeCN, Biosolve) was used as a coupling reagent and 3% dichloroacetic acid in 1,2-dichloroethane for the detritylation step. Coupling efficiency was estimated from a trityl assay and was >95%. After chain elongation and final detritylation, the oligomers were cleaved from the resin and deprotected by treatment with 1 cm^3 of conc. aq. ammonia solution (25%) at 55 °C during 16 h and filtered through syringe filters with a 0.45 μm GHP membrane (Pall). The ammonia solution was then removed by evaporation. The crude oligonucleotides were purified by reversed-phase HPLC with a Lichrocart column (250 × 10 mm) packed with Lichrospher RP 18 (10 μm) from Merck on a HPLC system using a linear gradient of acetonitrile from 0 to 30% over 30 min, in 0.1 M aq. triethylammonium acetate buffer, pH 7, with a flow rate of 4 cm^3 min^{-1} and detection at λ = 260 nm. After purification, the purity of all oligomers described was verified by reverse-phase analysis using a Lichrocart system (125 × 4 mm) packed with Lichrospher RP 18 (5 μm) from Merck eluted with a linear gradient of acetonitrile from 0 to 27.5% over 30 min in a 0.1 M aq. triethylammonium acetate buffer, pH 7, with a flow rate of 1 cm^3 min^{-1}. The integrity of all oligonucleotides was confirmed by MALDI-TOF mass spectrometry. The observed single-product ions were all within 0.1% of the calculated mass.

Physical studies

UV-melting curves. Solutions of duplexes (1 μM each strand) were prepared in a 10 mM NaH_2PO_4 buffer (pH 7.0) containing 150 mM NaCl and 1 mM EDTA. Thermal melting experiments were performed on an Uvikon 941 UV/VIS spectrophotometer equipped with a Ministat with a heating rate of 0.5 °C min^{-1}. T_m values were obtained by the baseline method.[68] The uncertainty of the T_m values reported was ±1 °C based on independent series of experiments.

Thermodynamic parameters. The thermodynamic parameters of the duplex formation for the modified ONs involving either a single (ONs **5** and **9**) or three modifications (ONs **6**, **7**, **10** and **11**) with both the DNA (ON **1**) and the RNA (ON **2**) targets were determined by a plot of $1/T_m$ *versus* log $[C_m]$.[51,52] C_m is the concentration of free ONs **5–7** and **9–11** at the melting temperature. ON concentrations were 10^{-5} M, 5×10^{-6} M, 2.5×10^{-6} M, and 10^{-6} M in a 10 mM NaH_2PO_4 buffer (pH 7.0) containing 150 mM NaCl and 1 mM EDTA. On the basis of the T_m values observed for different independent experiments, the uncertainty of the ΔG values can be estimated to be ±10%.

Circular dichroism spectroscopy. CD measurements were carried out on a Jasco J-810 spectropolarimeter. An optical cell with a path length of 0.1 cm was used. The temperature of the cell was adjusted with a Jasco PTC-4325 temperature controller at 10 ± 0.5 °C. Solutions of duplexes (4 μM each strand) were prepared in a 10 mM NaH_2PO_4 buffer (pH 7.0) containing 150 mM NaCl and 1 mM EDTA. The CD spectra were recorded between 215 and 315 nm. The reported spectra correspond to the average of three scans.

Molecular dynamic simulations. Initial structures of the DNA–DNA duplexes were generated with the nucleic acid builder (NAB) module of AMBER11[69] into a uniform ideal Watson/Crick B-form DNA duplex. Regarding the RNA–DNA duplex of the unmodified sequence, each strand was built following its ideal geometry (A-helix and B-helix for the RNA and DNA strand respectively), then both strands were combined to form a hybrid A–B duplex. The initial structures of the modified RNA–DNA duplexes were extracted from the MD simulation of the parent RNA–DNA duplex to allow the adjustment of the two strands together before inserting modifications. Geometry and charge distribution of modified nucleotides (Un and dU) were computed using the Jaguar program[70] at the HF/6-31G* level and fitted with the Resp program for compatibility with the Wang *et al*. force field[71] including parmbsc0 modifications.[72]

The SANDER module of the AMBER11 package was used for the simulations. All systems were neutralized with Na+ counter-ions and solvated with TIP3P water molecules. After 4000 steps of energy minimization, the system was heated from 0 K to 300 K with restraints applied on atomic positions of the oligomer and the counter-ions, then relaxed during 250 ps with gradual removal of the atomic restraints. A final

relaxation step of 10 ps was performed without any restraint, followed by 5 ns of free MD simulation in an NPT ensemble with periodic boundary conditions. The conformational parameters of nucleic acids were analyzed as time series using the program CURVES+[73] and the PTRAJ module of the AMBER11 package. To follow the evolution of the neopentyl group positioning during the simulation, we defined the Ω angle as the torsion angle $\{P_A, P_{Un}, O3'_{Un}, C_{Un}\}$ (Fig. 8 in ESI†).

Acknowledgements

A grant and post-doctoral funding (G. M.) from the Département du Loiret and post-doc co-funding (G. M.) from NucleoSyn are gratefully acknowledged. Analyses have been performed by the CBM and ICOA spectrometry facilities and Centre de Mesures physiques, Univ. B.P Clermont-Ferrand. We thank G. Gaband (CBM), Dr C. Colas (FR 2708 CBM/ICOA) and Dr B. Legeret (Univ BP, CF) for recording MS spectra, H. Meudal (CBM) and Dr M. Lefoix (NucleoSyn) for recording NMR spectra and Dr S. Villette (CBM) for her help in the T_m and CD experiments.

Notes and references

1 J. C. Burnett and J. J. Rossi, *Chem. Biol.*, 2012, **19**, 61.
2 B. L. Davison and P. B. McCray, *Nat. Rev. Genet.*, 2011, **12**, 329.
3 R. Garzon, G. Marcucci and C. M. Croce, *Nat. Rev. Drug Discovery*, 2010, **9**, 775.
4 C. R. Sibley, Y. Seow and M. J. A. Wood, *Mol. Ther.*, 2010, **18**, 466.
5 C. F. Bennett and E. E. Swayze, *Annu. Rev. Pharmacol. Toxicol.*, 2010, **50**, 259.
6 R. N. Veedu, B. Vester and J. Wengel, *Chem. Biodiversity*, 2010, **7**, 536.
7 P. E. Nielsen, *Chem. Biodiversity*, 2010, **7**, 786.
8 A. L. Jackson and P. S. Linsley, *Nat. Rev. Drug Discovery*, 2010, **9**, 57.
9 A. Pasternak and J. Wengel, *Org. Biomol. Chem.*, 2011, **9**, 3591.
10 K. Tiemann and J. J. Rossi, *EMBO Mol. Med.*, 2009, **1**, 142.
11 A. Forsbach, U. Samulowitz, K. Volp, H. P. Hofmann, B. Noll, S. Tluk, C. Schmitz, T. Wader, C. Muller, A. Podszuweit, A. Lohner, R. Curdt, E. Uhlmann and J. Vollmer, *Nucleic Acids Ther.*, 2011, **21**, 423.
12 J. K. Watts, G. F. Deleavey and M. J. Damha, *Drug Discovery Today*, 2008, **13**, 842.
13 R. Kole, A. R. Krainer and S. Altman, *Nat. Rev. Drug Discovery*, 2012, **11**, 125.
14 M. L. Stephenson and P. C. Zamecnik, *Proc. Natl. Acad. Sci. U. S. A.*, 1978, **75**, 285.
15 S. M. Elbashir, J. Harborth, W. Lendeckel, A. Yalcin, K. Weber and T. Tuschl, *Nature*, 2001, **411**, 494.
16 S. M. Freier and K.-H. Altman, *Nucleic Acids Res.*, 1997, **25**, 4429.
17 M. Egli and P. S. Pellan, *Annu. Rev. Biophys. Biomol. Struct.*, 2007, **36**, 281.
18 G. F. Deleavey, J. K. Watts, T. Alain, F. Robert, A. Kalota, V. Aishwarya, J. Pelletier, A. M. Gewirtz, N. Sonenberg and M. J. Damha, *Nucleic Acids Res.*, 2010, **38**, 4547.
19 J. D. Moulton and S. Jiang, *Molecules*, 2009, **14**, 1304.
20 J. K. Watts, G. F. Deleavey and M. J. Damha, *Drug Discovery Today*, 2008, **13**, 842.
21 D. Ittig, S. Luisier, J. Weiler, D. Schumperli and C. Leumann, *Artif. DNA PNA XNA*, 2010, **1**, 9.
22 A. L. Jackson, J. Burchard, D. Leake, A. Reynolds, J. Schelter, J. Guo, J. M. Johnson, L. Lim, J. Karpilow, K. Nichols, W. Marshall, A. Khvorova and P. S. Linsley, *RNA*, 2006, **12**, 1197.
23 K. Ui-Tei, Y. Naito, S. Zenno, K. Nishi, K. Yamato, F. Takahashi, A. Juni and K. Saigo, *Nucleic Acids Res.*, 2008, **36**, 2136.
24 M. Manoharan, A. Akinc, R. K. Pandey, J. Qin, P. Hadwiger, M. John, K. Mills, K. Charisse, M. A. Maeir, L. Nechev, E. M. Greene, P. S. Pallan, E. Rozners, K. G. Rajeev and M. Egli, *Angew. Chem., Int. Ed.*, 2011, **50**, 2284.
25 J. B. Bramsen, M. B. Laursen, A. F. Nielsen, T. B. Hansen, C. Bus, N. Langkjær, B. R. Babu, T. Hojland, M. Abramov, A. van Aerschot, D. Odadzic, R. Smicius, J. Haas, C. Andree, J. Barman, M. Wenska, P. Srivastava, C. Zhou, D. Honcharenko, S. Hess, E. Müller, G. V. Bobkov, S. N. Mikhailov, E. Fava, T. F. Meyer, J. Chattopadhyaya, M. Zerial, J. W. Engels, P. Herdewijn, J. Wengel and J. Kjems, *Nucleic Acids Res.*, 2009, **37**, 2867.
26 J. B. Bramsen, M. M. Pakula, T. B. Hansen, C. Bus, N. Langkjær, D. Odadzic, R. Smicius, S. L. Wengel, J. Chattopadhyaya, J. W. Engels, P. Herdewijn, J. Wengel and J. Kjems, *Nucleic Acids Res.*, 2010, **38**, 5761.
27 H. Addepalli, Meena, C. G. Peng, G. Wang, Y. Fan, K. Charisse, K. N. Jayaprakash, K. G. Rajeev, R. K. Pandey, G. Lavine, L. Zhang, K. Jahn-Hofmann, P. Hadwiger, M. Manoharan and M. A. Maier, *Nucleic Acids Res.*, 2010, **38**, 7320.
28 A. Pasternak and J. Wengel, *Nucleic Acids Res.*, 2010, **38**, 6697.
29 D. Ittig, A.-B. Gerber and C. J. Leumann, *Nucleic Acids Res.*, 2011, **39**, 373.
30 V. Tereshko, S. Portmann, E. C. Tay, P. Martin, F. Natt, K.-H. Altmann and M. Egli, *Biochemistry*, 1998, **37**, 10626.
31 K. E. Lind, V. Mohan, M. Manoharan and D. M. Fergusson, *Nucleic Acids Res.*, 1998, **26**, 3694.
32 P. S. Pallan, T. P. Prakask, F. Li, R. L. Eoff, M. Manoharan and M. Egli, *Chem. Commun.*, 2009, **2019**, 2017.
33 K. Yoshikawa, A. Ogata, C. Matsuda, M. Kohara, H. Iba, Y. Kitade and Y. Ueno, *Bioconjugate Chem.*, 2011, **22**, 42.
34 E. A. Lesnik and S. M. Freier, *Biochemistry*, 1998, **37**, 6691.
35 E. A. Lesnik, C. J. Guinosso, A. M. Kawasaki, H. Sasmor, M. Zounes, L. L. Cummins, D. J. Ecker, P. Dan Cook and S. M. Freier, *Biochemistry*, 1993, **32**, 7832.
36 L. Cummins, S. R. Owens, L. M. Risen, E. A. Lesnik, S. M. Freier, D. McGee, C. J. Guinosso and P. Dan Cook, *Nucleic Acids Res.*, 1995, **23**, 2019.

37 T. P. Prakash, A. M. Kawasaki, E. V. Wancewicz, L. Shen, B. P. Monia, B. S. Ross, B. Bhat and M. Manoharan, *J. Med. Chem.*, 2008, **51**, 2766.
38 J. F. Williams, S. C. Case-Green, K. Mir and E. M. Southern, *Nucleic Acids Res.*, 1994, **22**, 1365.
39 N. E. Broude, T. Sano, C. L. Smith and C. R. Cantor, *Proc. Natl. Acad. Sci. U. S. A.*, 1994, **91**, 3072.
40 H. Inoue, Y. Hayase, A. Imura, S. Iwai, K. Miura and E. Ohtsuka, *Nucleic Acids Res.*, 1987, **15**, 6131.
41 H. Saneyoshi, I. Okamoto, Y. Masaki, A. Ohkubo, K. Seio and M. Sekine, *Tetrahedron Lett.*, 2007, **48**, 8554.
42 B. S. Ross, R. H. Springer, Z. Tortorici and S. Dimock, *Nucleosides Nucleotides*, 1997, **16**, 1641.
43 U. Legorburu, C. B. Reese and Q. Song, *Tetrahedron*, 1999, **55**, 5635.
44 J. P. H. Verheyden, D. Wagner and J. G. Moffatt, *J. Org. Chem.*, 1971, **36**, 250.
45 S. H. Langer, S. Connell and I. Wender, *J. Org. Chem.*, 1957, **23**, 50.
46 Y. Aubert and U. Asseline, *Org. Biomol. Chem.*, 2004, **2**, 3496.
47 E. A. Lesnik and S. M. Freier, *Biochemistry*, 1995, **34**, 10807.
48 S. Nakano, M. Fujimoto, H. Hara and N. Sugimoto, *Nucleic Acids Res.*, 1999, **14**, 2957.
49 K. J. Breslauer, R. Frank, H. Blöcker and L. A. Marky, *Proc. Natl. Acad. Sci. U. S. A.*, 1986, **83**, 3746.
50 S. Wang and E. Kool, *Biochemistry*, 1995, **34**, 4125.
51 C. E. Longfellow, R. Kierzek and D. H. Turner, *Biochemistry*, 1990, **29**, 278.
52 L. A. Marky and K. J. Breslauer, *Biopolymers*, 1987, **26**, 1601.
53 H. C. Nelson, J. T. Finch, B. F. Luisi and A. Klug, *Nature*, 1987, **330**, 221.
54 M. Coll, C. A. Frederick, A. H. Wang and A. Rich, *Proc. Natl. Acad. Sci. U. S. A.*, 1987, **84**, 8385.
55 M. Katahira, H. Sugeta and Y. Kyogoku, *Nucleic Acids Res.*, 1990, **18**, 613.
56 M. Strahs and T. Schlick, *J. Mol. Biol.*, 2000, **301**, 643.
57 N. E. Mollegaard and P. E. Nielsen, *Biochemistry*, 2003, **42**, 8587.
58 A. M. Kawasaki, M. D. Casper, S. M. Freier, E. A. Lesnik, M. C. Zounes, L. L. Cummins, C. Gonzalez and P. D. Cook, *J. Med. Chem.*, 1993, **36**, 831.
59 D. M. Williams, F. Benseler and F. Eckstein, *Biochemistry*, 1991, **30**, 4001.
60 T. P. Prakash, M. Manoharan, A. S. Frase, A. S. Kawasaki, E. A. Lesnik and S. R. Owens, *Tetrahedron Lett.*, 2000, **41**, 4855.
61 A. M. Soto, B. I. Kankia, P. Dande, B. Gold and L. A. Marky, *Nucleic Acids Res.*, 2002, **30**, 3171.
62 T. P. Prakash, A. Puschl, E. Lesnik, V. Mohan, V. Tereshko, M. Egli and M. Manoharan, *Org. Lett.*, 2004, **6**, 1971.
63 M. Egli, G. Minasov, V. Tereshko, P. S. Pallan, M. Teplova, G. B. Inamati, E. A. Lesnik, S. R. Owens, B. R. Ross, T. P. Prakash and M. Manoharan, *Biochemistry*, 2005, **44**, 9045.
64 A. A. Koshkin, S. K. Singh, P. Nielsen, V. K. Rajwanshi, R. Kumar, M. Meldgaard, C. E. Olsen and J. Wengel, *Tetrahedron*, 1998, **54**, 3607.
65 H. Kaur, J. Wengel and S. Maiti, *Biochemistry*, 2008, **47**, 1218.
66 M. Egli, G. Minasov, V. Tereshko, P. S. Pallan, M. Teplova, G. B. Inamati, E. A. Lesnik, S. R. Owens, B. R. Ross, T. P. Prakash and M. Manoharan, *Biochemistry*, 2005, **44**, 9045.
67 C. R. Cantor, M. M. Warshaw and H. Shapiro, *Biopolymers*, 1970, **9**, 1059.
68 J.-L. Mergny and L. Lacroix, *Oligonucleotides*, 2003, **13**, 515.
69 D. A. Case, T. A. Darden, T. E. Cheatham III, C. L. Simmerling, J. Wang, R. E. Duke, R. Luo, R. C. Walker, W. Zhang, K. M. Merz, B. Roberts, B. Wang, S. Hayik, A. Roitberg, G. Seabra, I. Kolossváry, K. F. Wong, F. Paesani, J. Vanicek, J. Liu, X. Wu, S. R. Brozell, T. Steinbrecher, H. Gohlke, Q. Cai, X. Ye, J. Wang, M.-J. Hsieh, G. Cui, D. R. Roe, D. H. Mathews, M. G. Seetin, C. Sagui, V. Babin, T. Luchko, S. Gusarov, A. Kovalenko and P. A. Kollman, *AMBER 11*, University of California, San Francisco, 2010.
70 *Jaguar, version 7.8*, Schrödinger, LLC, New York, NY, 2011.
71 J. Wang, P. Cieplak and P. A. Kollman, *J. Comput. Chem.*, 2000, **21**, 1049.
72 A. Perez, I. Marchan, D. Svozil, J. Sponer, T. E. Cheatham, C. A. Laughton and M. Orozco, *Biophys. J.*, 2007, **92**, 3817.
73 R. Lavery, M. Moakher, J. H. Maddocks, D. Petkeviciute and K. Zakrewska, *Nucleic Acids Res.*, 2009, **37**, 5917.